Vilnius
University
Press

Pulsating hydromagnetic flow of Au-blood micropolar nanofluid in a channel with Ohmic heating, thermal radiation and heat source/sink

Devendiran Rajkumar[iD], **Anala Subramanyam Reddy**[iD]

Department of Mathematics, School of Advanced Sciences,
Vellore Institute of Technology, Vellore-632014, India
anala.subramanyamreddy@gmail.com

Abstract. The current work deals with the pulsating flow of Au-blood micropolar nanofluid with the existence of thermal radiation and Joule heating. Micropolar fluid is addressed as blood (base fluid) and Au (gold) as a nanoparticle. The flow has been mathematically modeled, resulting in a delicate system of partial differential equations (PDEs). A perturbation technique is used to convert the PDE system into ordinary differential equations (ODEs), which are subsequently solved by using the shooting method with the Runge–Kutta fourth-order scheme. The effects of various parameters on the velocity, microrotation, temperature, and heat transfer rate of Au-blood nanofluid are graphically depicted and explored successively. The obtained findings bring out that the velocity of nanofluid decreases over a rise in the coupling parameter, magnetic field, and nanoparticle volume fractions. The temperature is reducing with an increment of radiation parameter, frequency parameter, coupling parameter, magnetic field, and volume fraction of nanoparticles. Further, the results show that the Nusselt number against frequency distribution increasing with the rising values of the Eckert number.

Keywords: pulsatile flow, micropolar nanofluid, Joule heating, Hartmann number, thermal radiation.

1 Introduction

In 1966, Eringen [12] introduced the theory of the micropolar fluid model and later extended it into a thermo-micropolar fluid. The non-Newtonian micropolar fluid is characterized by microstructures, rigid and randomly focused particles on microrotation of fluid components. Such fluid is taken into account through macroscopic views such as polymeric fluids, liquid crystals, colloidal suspensions, animal and human blood. Blood is a nonhomogeneous fluid that streams inside the human artery system and delivers the cells with nutrients due to the blood's microstructure, and its flow inside a human carotid model can be taken as micropolar fluid. Eringen have established the micropolar fluid model for viscoplastic and viscoelastic medium containing through a classical continuum

and thermodynamics. He formulated a much complex structure for simulating effective microrheological properties and areas of applications in various industrial and engineering fields like chemical engineering, arterial blood flows, synovial fluid, biofluids, semicircular canal fluids, gastric liquids, slurry technologies. Nowadays, a micropolar theory has been successfully performed in various branches in the medical field [5, 7, 13, 20, 25]. Sheikholeslami et al. [27] discussed the effects of substantial parameters like microrotation and angular velocity, Reynolds number, Peclet number then solved laminar flow of steady micropolar fluid on porous walls of two-dimensional channel. Rashad et al. [24] probed the heat transfer and convective flow of micropolar nanofluids on a cylinder in a soaked penetrable medium. Kabeir et al. [10] investigated the hydromagnetic flow of micropolar ferrofluid with thermal radiation and partial slip effects. Mahdy et al. [17] scrutinized the convective flow of a micropolar hybrid nanofluid with the presence of internal heat generation, magnetic field, and thermal radiation. Rashad et al. [23] studied the coupled heat and mass transfer and the influence of chemical reaction through a combined convectional micropolar fluid. Bhattacharyya et al. [3] analytically investigated the heat transfer on the flow of carbon nanotubes between two expandable coaxial rotating disks subject to the Cattaneo–Christov heat flux model by employing optimal homotopy analysis method. Motivated by the aforesaid studies, it is noticed that there is a gap related to the survey of the pulsating flow of micropolar nanofluid into a channel with the presence of applied magnetic field, Joule heating, viscous dissipation. So that, in this analysis, we made an attempt to study the simultaneous impacts of viscous dissipation and Joule heating on pulsating magnetohydrodynamic (MHD) flow of a micropolar nanofluid with the influence of heat source/sink and thermal radiation.

The investigation of pulsating flow in a channel turns out to be the aim of scientific exploration due to its significance on biological demands, which is corresponding to hemodynamics, and the several researchers have attracted due to their technological systems like circulatory systems, gaseous diffusion, transpiration cooling, and respiratory system [2, 6, 18, 19, 21, 33]. The pulsatile flow, which is the rate of fluid flow that stimulates by a periodic oscillation or pressure gradient and the superimposed periodical time-varying component, is composed into a steady flow component. The mathematical analysis is divided into two sections, one dealing with higher-order outcomes for the microinertia, microstretch, and micropressure fields, as well as the other with solutions for the velocity and microrotation fields. The pulsatile flow of microstretch fluids in circular tubes is studied as a result of a sinusoidally changing pressure gradient. Venkatesan and Reddy [31] analyzed the effects of pulsatile flow of blood-alumina nanofluid in a channel with the existence of viscous dissipation and Joule heating. Bitla and Iyengar [4] examined the pulsating flow of noncompressible micropolar fluid in the middle of porous walls with an angled magnetic field by adopting the perturbation method. Srinivas et al. [28] investigated the chemical and Soret impacts on the hydromagnetic pulsatile flow of Casson fluid into the permeable channel.

In the present days, the study of nanofluid is greatly essential due to its significant implementations in electronic, optical, and biomedical fields. Nanofluids are a comparatively current category of heat transfer that has fascinated much observation of researchers from previous generations around the globe [22, 30]. The section of nanofluids was first

established by Choi [9] in 1995. Nanofluid is a fluid that contains nanosized (less than 100 nm) solid particles in the base fluid. Many scientists have been observed extraordinary thermal characteristics in nanofluids and developed a new model. The good compilation of issued papers on nanofluids can be discovered in the book by Choi [8]. Selimefendigil et al. [26] performed the numerical study of forced convective nanofluid flow in a bifurcating channel with the existence of a uniform magnetic field by adopting the Galerkin weighted residual finite element method. Hashmi et al. [14] analytically discussed the problem of MHD squeezing flow of a nanofluid between two disks employing homotopy analysis approach. Vijayalakshmi et al. [32] investigated the hydromagnetic pulsating flow of nanofluids between parallel walls, and the authors treated water as base fluid, and silver, alumina, titanium dioxide, and copper oxide are indicated as nanoparticles. Hatami et al. [15] pointed out the features of gold-blood nanofluid flow through a hollow vessel in the existence of a magnetic field. Elgazery [11] presented the flow of a blood-based non-Newtonian nanofluid with alumina and gold nanoparticles via the non-Darcian penetrable medium. Reddy et al. [29] highlighted the thermal properties of Au/Cu-blood nanofluid flow through a permeable channel with stretching or shrinking walls for its heat transfer properties. Abo-Dahab et al. [1] interrogated the hydromagnetic Casson nanofluid flow in a permeable medium with the transversal magnetized field and suction/injection effects. Kumar et al. [16] exhibited the pulsatile flow characteristics of Casson nanofluid into an allowable channel with help of the perturbation method.

Propelled by the above literature survey, it is noticed that no attempt related to the survey of the pulsating flow of micropolar nanofluid into a channel with the applied magnetic field, Joule heating, viscous dissipation effects has made so far. The current work aims to look at the simultaneous impacts of viscous dissipation and Joule heating on pulsating MHD flow of a micropolar nanofluid with the influence of heat source/sink and thermal radiation. The present study may be useful in the study of physical aspects of biomedical, drug delivery, or radio therapy using nanoparticles. In the present work, blood is taken as micropolar fluid (base fluid), and gold (Au) is chosen as a nanoparticle. Gold nanoparticles are efficient in drug carry and drug delivery vehicles because they can encapsulate large quantities of therapeutic molecules. Here the perturbation technique is utilized to convert a set of partial differential equations (PDEs), which are governing current flow into a set of ordinary differential equations (ODEs) and then numerically solved by employing the shooting technique and the Runge–Kutta fourth-order procedure. The velocity, temperature, and rate of heat transfer distributions of micropolar nanofluid are discussed via pictorial representations in detail.

2 Formulation of the problem

We consider an incompressible and laminar pulsatile flow of electrically conducting micropolar nanofluid through a channel. The schematic diagram of the current flow model is exhibited in Fig. 1. Assume that the bottom wall is parallel to the x^*-axis and that the y^*-axis is perpendicular to it. Micropolar fluid is taken as blood (base fluid), and gold (Au) as a nanoparticle. The Joule heating, viscous dissipation, thermal radiation, and heat
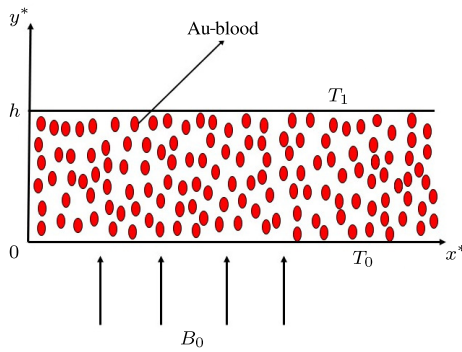
Figure 1. Physical model for flow problem.

source/sink are taken into account. An applied magnetic field of magnitude B_0 is enforced uniformly orthogonal to both the walls. Since no external electric field is applied and the effect of polarization of the ionized fluid is negligible, we can assume that the electric field is zero. When the external electric field is zero and the induced electric field is negligible, the magnetic Reynolds number is very small; so that effects of both the Hall effect and the induced magnetic field are negligible compared with the applied magnetic field. The bottom and top walls are retained at consistent temperatures T_0 and T_1, respectively. Under these hypothesis, the governing equations are given by [4, 5, 27, 32]:

$$\frac{\partial u^*}{\partial t^*} = -\frac{1}{\rho_{nf}}\frac{\partial P^*}{\partial x^*} + \frac{K_1}{\rho_{nf}}\frac{\partial N^*}{\partial y^*} + \left(\frac{\mu_{nf} + K_1}{\rho_{nf}}\right)\frac{\partial^2 u^*}{\partial y^{*2}} - \frac{\sigma_{nf}B_0^2}{\rho_{nf}}u^*, \qquad (1)$$

$$\frac{\partial N^*}{\partial t^*} = -\frac{1}{\rho_{nf}j}2K_1 N^* - \frac{K_1}{\rho_{nf}j}\frac{\partial u^*}{\partial y^*} + \frac{\gamma}{\rho_{nf}j}\frac{\partial^2 N^*}{\partial y^{*2}}, \qquad (2)$$

$$\frac{\partial T^*}{\partial t^*} = \frac{k_{nf}}{(\rho C_p)_{nf}}\frac{\partial^2 T^*}{\partial y^{*2}} + \frac{\mu_{nf} + K_1}{(\rho C_p)_{nf}}\left(\frac{\partial u^*}{\partial y^*}\right)^2 + \frac{\sigma_{nf}B_0^2}{(\rho C_p)_{nf}}u^{*2}$$
$$- \frac{1}{(\rho C_p)_{nf}}\frac{\partial q_r}{\partial y^*} + \frac{Q_0}{(\rho C_p)_{nf}}(T^* - T_0). \qquad (3)$$

Here u^* is velocity along with in x^*-direction, P^* is the fluid pressure. ρ_{nf}, μ_{nf}, σ_{nf}, $(\rho C_p)_{nf}$, and k_{nf} represent density, dynamic viscosity, electrical conductivity, effective specific heat, and thermal conductivity of nanofluid, accordingly, and the subscripts nf, f, and s denote the nanofluid, base fluid, and solid nanoparticles, respectively. T^* is the temperature of nanofluid, K_1 is coupling parameter, N^* is microrotation vector, j is microinertia parameter, q_r is the radiative heat flux, and Q_0 is the coefficient of the heat source/sink.

The corresponding boundary conditions (BCs) are

$$\begin{aligned}
u^*(0) &= 0, & N^*(0) &= 0, & T^*(0) &= T_0, \\
u^*(h) &= 0, & N^*(h) &= 0, & T^*(h) &= T_1.
\end{aligned} \qquad (4)$$

Here h is the distance between the walls.

Table 1. The thermal features of Au nanoparticles
and blood [11, 15].

Property	Au	Blood
k (W/mK)	318	0.52
C_p (J/kg K)	129	3617
ρ (kg/m^3)	19300	1050
σ (Ω m)$^{-1}$	$4.10 \cdot 10^7$	0.8

The characteristics of nanofluid are defined as [15, 29]

$$(\rho C_p)_{nf} = (1 - \phi)(\rho C_p)_f + \phi(\rho C_p)_s; \qquad \rho_{nf} = (1 - \phi)\rho_f + \phi\rho_s;$$

$$\mu_{nf} = \frac{\mu_f}{(1 - \phi)^{2.5}}; \qquad \frac{k_{nf}}{k_f} = \frac{k_s + 2k_f - 2\phi(k_f - k_s)}{k_s + 2k_f + \phi(k_f - k_s)};$$

$$\frac{\sigma_{nf}}{\sigma_f} = 1 + \frac{3(\frac{\sigma_s}{\sigma_f} - 1)\phi}{(\frac{\sigma_s}{\sigma_f} + 2) - (\frac{\sigma_s}{\sigma_f} - 1)\phi}. \tag{5}$$

Here ϕ is volume fraction of nanoparticles. The thermal features of base fluid and nanoparticles are shown in Table 1.

Now, with the help of Rosseland approximation for the radiative heat flux q_r, Eq. (3) becomes

$$\frac{\partial T^*}{\partial t^*} = \frac{k_{nf}}{(\rho C_p)_{nf}} \frac{\partial^2 T^*}{\partial y^{*2}} + \frac{1}{(\rho C_p)_{nf}} \left[\frac{16\sigma^*}{3k^*} T_1^3 \frac{\partial^2 T^*}{\partial y^{*2}} \right] + \frac{\mu_{nf} + K_1}{(\rho C_p)_{nf}} \left(\frac{\partial u^*}{\partial y^*} \right)^2$$

$$+ \frac{\sigma_{nf} B_0^2}{(\rho C_p)_{nf}} u^{*2} + \frac{Q_0}{(\rho C_p)_{nf}}(T^* - T_0). \tag{6}$$

By utilizing the ensuing nondimensionl parameters,

$$u = \frac{u^*}{U}, \qquad N = \frac{N^* h}{U}, \qquad x = \frac{x^*}{h}, \qquad y = \frac{y^*}{h},$$

$$t = \omega t^*, \qquad P = \frac{h P^*}{\mu_f U}, \qquad \theta = \frac{T^* - T_0}{T_1 - T_0}. \tag{7}$$

Equations (1), (2), and (6) become

$$R^2 \frac{\partial u}{\partial t} = -\frac{1}{A_1} \frac{\partial P}{\partial x} + \frac{K}{A_1} \frac{\partial N}{\partial y} + \left(\frac{A_2 + K}{A_1} \right) \frac{\partial^2 u}{\partial y^2} - \frac{A_5}{A_1} M^2 u, \tag{8}$$

$$P_j R^2 \frac{\partial N}{\partial t} = -\frac{2nN}{A_1} - \frac{n}{A_1} \frac{\partial u}{\partial y} + \frac{1}{A_1} \frac{\partial^2 N}{\partial y^2}, \tag{9}$$

$$R^2 \frac{\partial \theta}{\partial t} = \left(\frac{A_4}{A_3} + \frac{4}{3} \frac{Rd}{A_3} \right) \frac{1}{Pr} \frac{\partial^2 \theta}{\partial y^2} + \left(\frac{A_2}{A_3} + K \right) Ec \left(\frac{\partial u}{\partial y} \right)^2$$

$$+ \left(\frac{A_5}{A_3} Ec \right) M^2 u^2 + \frac{Q}{A_3} \theta. \tag{10}$$

Here

$$A_1 = (1 - \phi) + \phi \frac{\rho_s}{\rho_f}, \qquad A_2 = \frac{1}{(1 - \phi)^{2.5}}, \qquad A_3 = (1 - \phi) + \phi \frac{(\rho C_p)_s}{(\rho C_p)_f},$$

$$A_4 = \frac{k_s + 2k_f - 2\phi(k_f - k_s)}{k_s + 2k_f + \phi(k_f - k_s)}, \qquad A_5 = 1 + \frac{3(\frac{\sigma_s}{\sigma_f} - 1)}{(\frac{\sigma_s}{\sigma_f} + 2) - (\frac{\sigma_s}{\sigma_f} - 1)\phi},$$

$Pr = (\rho C_p)_f \nu_f / k_f$ is the prandtl number, $Ec = U^2/((C_p)_f(T_1 - T_0))$ is the Eckert number, $R^2 = \omega h^2/\nu_f$ is the frequency parameter, $M = B_0 h \sqrt{\sigma_f/\mu_f}$ is Hartmann number, $K = K_1/\mu_f$ is coupling parameter, $Rd = 4\sigma^* T_1^3/(k_f k^*)$ is the radiation parameter, $n = K_1 h^2/\gamma$ is gyration parameter, $P_j = j\mu_f/\gamma$ is microinertia parameter, $Q = Q_0 h^2/((\rho C_p)_f \nu_f)$ is the heat source/sink parameter.

The appropriate BCs are

$$\begin{aligned} u(0) = 0, \qquad N(0) = 0, \qquad \theta(0) = 0, \\ u(1) = 0, \qquad N(1) = 0, \qquad \theta(1) = 1. \end{aligned} \tag{11}$$

3 Solution of the problem

The pressure gradient of the form is supposed to induce the pulsating flow

$$-\frac{\partial P}{\partial x} = \lambda_0 + \varepsilon \lambda_1 e^{it}. \tag{12}$$

Since the pressure gradient conferred in Eq. (12) causes the flow of velocity, microrotation and temperature are declared as

$$u = u_0(y) + \varepsilon u_1(y)e^{it}, \qquad N = N_0(y) + \varepsilon N_1(y)e^{it}, \qquad \theta = \theta_0(y) + \varepsilon \theta_1(y)e^{it}. \tag{13}$$

By substituting Eqs. (12)–(13) in Eqs. (8)–(10) and equating the coefficients of like power of ε, one can acquire

$$\left(\frac{A_2 + K}{A_1}\right)\frac{d^2 u_0}{dy^2} - \left(\frac{A_5}{A_1}\right)M^2 u_0 + \frac{K}{A_1}\frac{dN_0}{dy} = -\frac{\lambda_0}{A_1}, \tag{14}$$

$$\left(\frac{A_2 + K}{A_1}\right)\frac{d^2 u_1}{dy^2} - \left(\frac{A_5}{A_1}M^2 + R^2 i\right)u_1 + \frac{K}{A_1}\frac{dN_1}{dy} = -\frac{\lambda_1}{A_1}, \tag{15}$$

$$\left(\frac{1}{A_1}\right)\frac{d^2 N_0}{dy^2} - \left(\frac{2n}{A_1}\right)N_0 - \left(\frac{n}{A_1}\right)\frac{du_0}{dy} = 0, \tag{16}$$

$$\left(\frac{1}{A_1}\right)\frac{d^2 N_1}{dy^2} - \left(\frac{2n}{A_1} + P_j R^2 i\right)N_1 - \frac{n}{A_1}\frac{du_1}{dy} = 0, \tag{17}$$

$$\frac{1}{Pr}\left(\frac{A_4}{A_3} + \frac{4}{3}\frac{Rd}{A_3}\right)\frac{d^2 \theta_0}{dy^2} + \left(\frac{A_2}{A_3} + K\right)Ec\left(\frac{du_0}{dy}\right)^2$$
$$+ \left(\frac{A_5}{A_3}EcM^2\right)u_0^2 + \frac{Q}{A_3}\theta_0 = 0, \tag{18}$$

$$\frac{1}{Pr}\left(\frac{A_4}{A_3} + \frac{4}{3}\frac{Rd}{A_3}\right)\frac{\mathrm{d}^2\theta_1}{\mathrm{d}y^2} - R^2\mathrm{i}\theta_1 + 2\left(\frac{A_2}{A_3} + K\right)Ec\frac{\mathrm{d}u_0}{\mathrm{d}y}\frac{\mathrm{d}u_1}{\mathrm{d}y}$$
$$+ 2\left(\frac{A_5}{A_3}EcM^2\right)u_0u_1 + \frac{Q}{A_3}\theta_1 = 0. \tag{19}$$

The corresponding BCs are

$$\begin{aligned}u_0 = 0, \quad N_0 = 0, \quad \theta_0 = 0, \quad u_1 = 0, \quad N_1 = 0, \quad \theta_1 = 0 \quad \text{at } y = 0,\\ u_0 = 0, \quad N_0 = 0, \quad \theta_0 = 1, \quad u_1 = 0, \quad N_1 = 0, \quad \theta_1 = 0 \quad \text{at } y = 1.\end{aligned} \tag{20}$$

Further, the nondimensionl heat transfer rate (Nusselt number) at the walls is assigned as

$$Nu = A_4\left[\left(\frac{\mathrm{d}\theta_0}{\mathrm{d}y}\right)_{y=0,1} + \varepsilon\mathrm{e}^{\mathrm{i}t}\left(\frac{\mathrm{d}\theta_1}{\mathrm{d}y}\right)_{y=0,1}\right]. \tag{21}$$

The system of Eqs. (14)–(19) is solved with boundary conditions (20) by adopting the shooting technique with Runge–Kutta fourth-order approach. The step size is fixed as 0.001 (i.e., $\Delta y = 0.001$). $1 \cdot 10^{-10}$ accuracy is fixed for the convergence criteria.

The comparison with the results of Venkatesan and Reddy [31] for $(\theta_0')_{y=0}$ and $(\theta_1')_{y=0}$ for Al_2O_3 nanoparticle is presented in Table 2. The comparison shows that there is a good agreement between the present results and the results of Venkatesan and Reddy [31]. Further, to check the correctness of the present results, we made a comparison between the present results and the results obtained by NDsolve using MATHEMATICA software, which are given in Table 3. It is observed that there is a good agreement between the present results and the results obtained by NDsolve.

Advantages and limitations of shooting method

The shooting method works by considering the boundary conditions as a multivariate function of initial conditions at some point, reducing the boundary value problem to

Table 2. Comparison with the results of Venkatesan and Reddy [31] for θ_0' and θ_1' at $y = 0$ with the presence of Al_2O_3 for different values of Ec, M, and Rd when $R = 1$, $M = 1$, $Pr = 21$, $Ec = 1$, $Rd = 1$, $t = \pi/3$, $\lambda_0 = 1$, $\lambda_1 = 1$, $K = 0$, $n = 0$, and $P_j = 0$.

Parameter	Values	Venkatesan–Reddy [31]		Present results	
		$(\theta_0')_{y=0}$	$(\theta_1')_{y=0}$	$(\theta_0')_{y=0}$	$(\theta_1')_{y=0}$
Ec	0.1	2.3652	0.0423	2.36308	0.04211
	0.3	2.4456	0.1270	2.44260	0.12634
	0.5	2.5260	0.2117	2.52211	0.21057
M	1	2.5260	0.2117	2.52211	0.21057
	2	2.4966	0.1638	2.49307	0.16310
	3	2.4625	0.1189	2.45931	0.11860
Rd	1	2.5260	0.2117	2.52211	0.21057
	2	1.7822	0.1697	1.77668	0.16819
	3	1.5254	0.1355	1.52092	0.13383

Table 3. Comparison of present and NDsolve results for heat transfer rate at $y = 0$ for different values of R, Q, and M when $t = \pi/2$, $Pr = 21$, $K = 1$, $R = 2$, $Ec = 1$, $Rd = 2$, $Q = -2$, and $\phi = 0.05$.

Parameter	Values	$(Nu)_{y=0}$	
		Present results	NDsolve
R	1	0.68935	0.68926
	2	0.68955	0.68946
	3	0.68959	0.68950
Q	-1	0.99716	0.99787
	-1.5	0.81460	0.81444
	-2	0.68955	0.68946
M	0	0.77193	0.77372
	2	0.68955	0.68946
	4	0.55061	0.54754

finding the initial conditions that give a root. The advantage of the shooting method is that it takes advantage of the speed and adaptivity of methods for initial value problems. The limitations of the method is that it is not as robust as finite difference or collocation methods: some initial value problems with growing modes are inherently unstable even though the BVP itself may be quite well posed and stable.

4 Results and discussion

In the present section, numerical simulations are used to test the dominant features of the flow behaviour of nanofluid. The static values of $t = \pi/2$, $M = 2$, $R = 2$, $K = 1$, $Ec = 1$, $n = 1$, $Rd = 2$, $Q = 1$, $Pr = 21$, $\lambda_0 = 1$, and $\lambda_1 = 1$ are considered for graphical results unless otherwise stated. The current scenario deals with the impacts of several parameters on velocity, microrotation, temperature, and Nusselt number (heat transfer rate) of Au-blood micropolar nanofluid with the help of graphical outcomes, which are presented in Figs. 2–7.
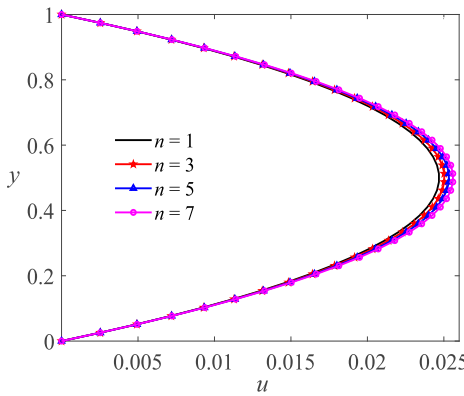
4.1 Velocity distribution

The velocity distributions for various values of coupling parameter (K), gyration parameter (n), Hartmann number (M), nanoparticles volume fraction (ϕ), and frequency parameter (R) are shown in Figs. 2(a)–2(e). Figure 2(a) exhibits the variations of the velocity of nanofluid with different values of coupling parameter (K). From Fig. 2(b) one can notice that the velocity falls with the enhancement of Hartmann number (M). The reason for the fall in the velocity is because of the retarding forces upon the utilization of magnetic field, which act opposite to the flow direction. Hence there is a fall in velocity. Figure 2(c) presents the impact of gyration parameter (n) on the velocity of nanofluid. This figure shows that the velocity is increasing with a rise of the gyration parameter. Figure 2(d) describes that the velocity slows down with the enhancement of nanoparticle volume fraction (ϕ). The reason behind this is the combined influence of thermal
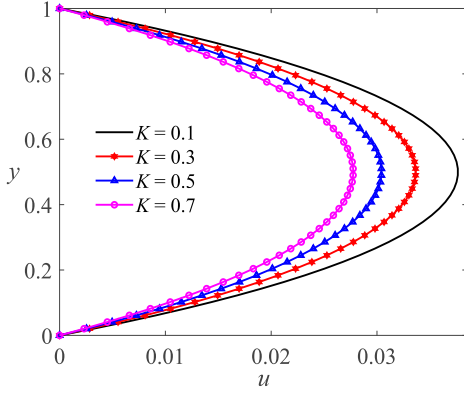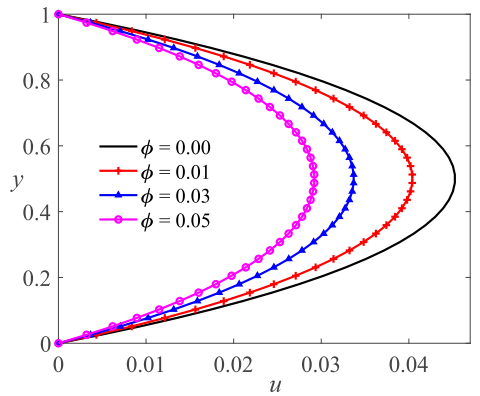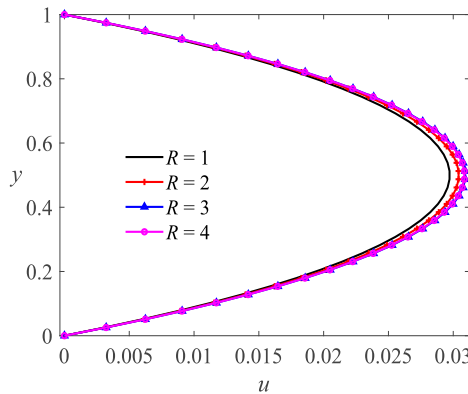
(a) Impact of K
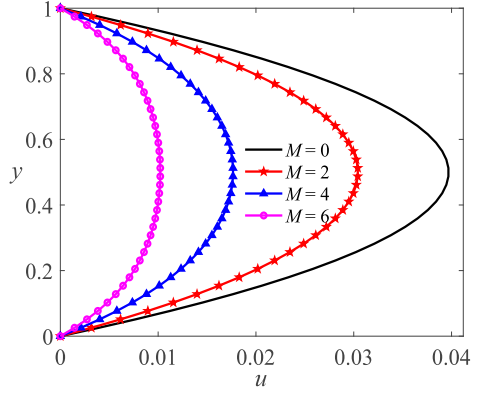
(b) Impact of M

(c) Impact of n

(d) Impact of ϕ

(e) Impact of R

Figure 2. Impact of various parameters K, M, n, ϕ, and R on the velocity distribution.

coefficient and density extension of the base fluid with nanoparticle mass density is signified. Figure 2(e) elucidates that there is an enhancement in the velocity of nanofluid with an increment on frequency parameter (R).

4.2 Microrotation distribution

The influence of coupling parameter (K), Hartmann number (M), gyration parameter (n), nanoparticles volume fraction (ϕ) on microrotation is presented in Figs. 3(a)–3(d). Figures 3(a) and 3(b) describe that the micro velocity is increasing near the bottom wall at the same time it is falling at the top wall by varying (K) and (M). Figure 3(c) demonstrates that by varying the gyration parameter (n) the microrotation velocity is decreasing near a bottom wall when it rising at the top wall. The opposite trend can be noticed from Fig. 3(d) by varying volume fractions (ϕ).
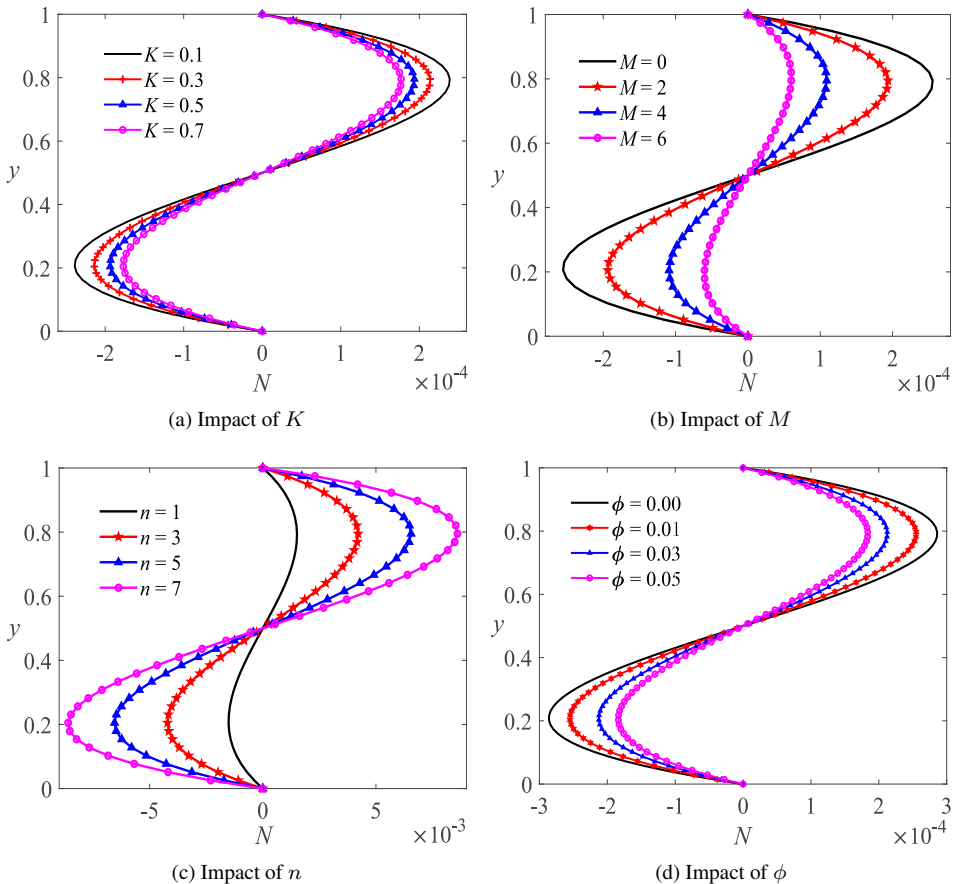

Figure 3. Impact of various parameters K, M, N, and ϕ on the microrotation distribution.

4.3 Temperature distribution

Figures 4(a)–4(d) and 5 are presented to see the impacts of Eckert number (Ec), radiation parameter (Rd), heat source/sink parameter (Q), coupling parameter (K), Hartmann number (M) on the profiles of temperature distribution (θ) of the nanofluid. Figure 4(a) displays that the temperature accelerates with an enhancement in Eckert number. Because Ec is correlated between the heat enthalpy and differences in kinetic energy, when we increase Ec, it leads to boost the kinetic energy of particles by reducing enthalpy factor, which rises the temperature. Figure 4(b) describes that there is a decrease in temperature distributions for the rising values of (Rd). Such decrease may be due to the physical fact that rising the radiation parameter reduces the thickness of the thermal boundary layer. Figure 4(c) reveals the temperature differences for various heat source/sink parameter values. It is clear that the temperature boosts up with the rising of heat source ($Q > 0$) due to the heat generation in the working nanofluid, while it reduces with enhancing of a heat
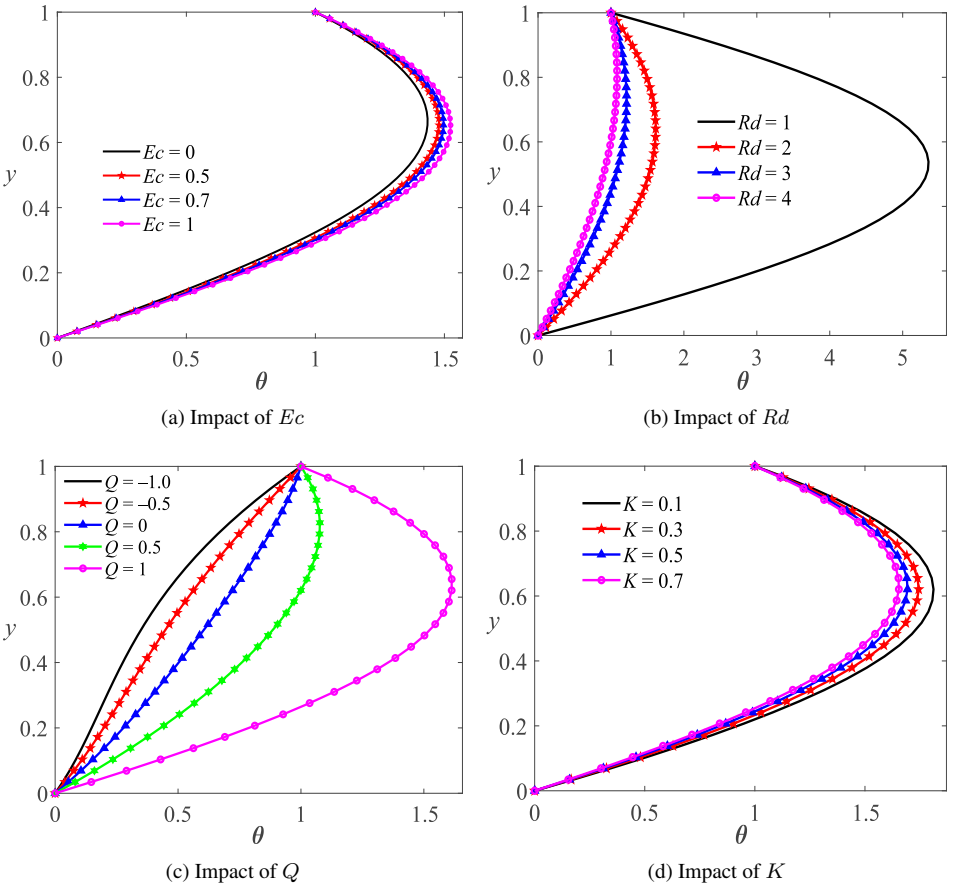

(a) Impact of Ec

(b) Impact of Rd

(c) Impact of Q

(d) Impact of K

Figure 4. Impact of various parameters Ec, Rd, Q, and K on the temperature distribution.
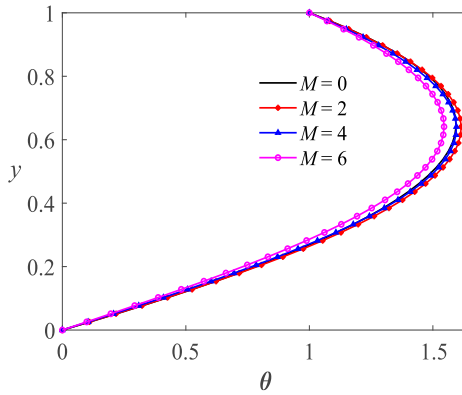
Figure 5. Impact of M on the temperature distribution.

sink ($Q < 0$) due to the heat amalgamation. Figure 4(d) shows that the temperature is decreasing, while the coupling parameter (K) increases. Because the coupling parameter is against the flow of temperature profile, this results in the decrease in θ. Figure 5 presents that increasing Hartmann number (M) decreases the temperature, this is maybe due to the Lorentz force effect created by applied an magnetic field, which reduces the thermal boundary layer thickness.

4.4 Nusselt distribution

Figures 6(a), 6(b), and 7(a)–7(c) depict the behaviour of the rate of heat transfer (Nu) of Au-blood nanofluid at the bottom wall ($y = 0$) against R for various parameters Ec, ϕ, M, Rd, and K. From these figures it is noticed that the rate of heat transfer is increasing function of R. Figure 6(a) elucidates that the heat transfer rate is rising
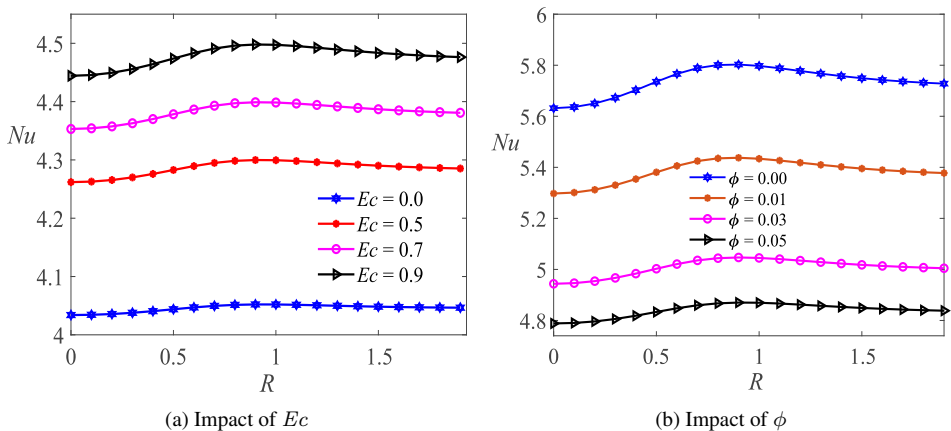

(a) Impact of Ec

(b) Impact of ϕ

Figure 6. Impact of various parameters Ec and ϕ on Nusselt number distribution.

(a) Impact of M

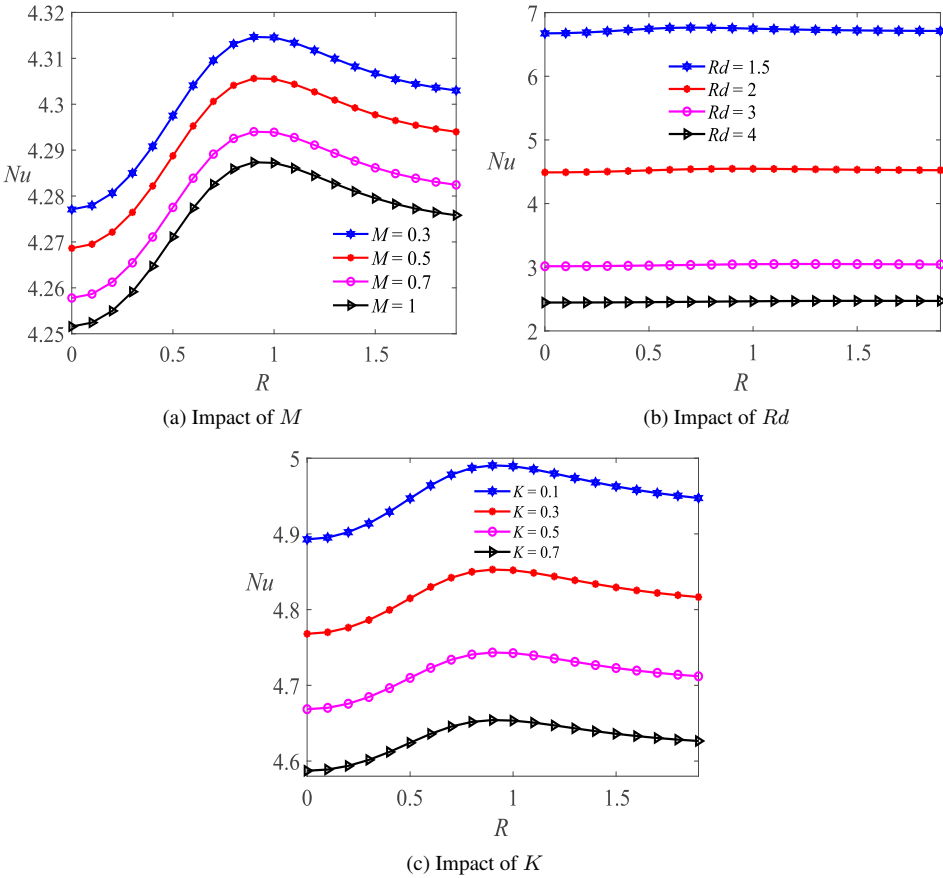(b) Impact of Rd

(c) Impact of K

Figure 7. Impact of various parameters M, Rd, and K on Nusselt number distribution.

with a rise in Ec. It is due to enhancing viscous dissipation accelerates the rate of heat transfer on the wall. Figure 6(b) presents that the Nusselt number is decreasing with an increment of nanoparticle volume fraction (ϕ). A similar trend is seen from Figs. 7(a)–7(c) with an improvement of Hartmann number, radiation parameter, and coupling parameter, respectively.

5   Conclusion

The current study investigates the pulsating MHD flow of Au-blood micropolar nanofluid in a channel with the presence of Joule heating and thermal radiation. Micropolar fluid is chosen as blood (base fluid) and gold (Au) as nanoparticles. The considered model is important in the study of biological fluid modeling, polymer engineering, sediments in rivers, and nanodrug delivery. The numerical results for dimensionless fluid flow variables are obtained by hiring a shooting technique with the aid of Runge–Kutta fourth-

order scheme. The impacts of relevant parameters on the velocity, microrotation, and temperature distributions of Au-blood nanofluid are investigated in detail by plotting graphs. The main outcomes are outlined as follows:

- Strengthening magnetic field dwindling the current flow due to the Lorentz forces produced by an applied magnetic field, which act opposite to the flow direction.
- The velocity of nanofluid is reducing with an enhancement of coupling parameter and nanoparticles volume fraction.
- The velocity is increasing with an enhancement of the gyration parameter and frequency parameter.
- The temperature profile is rising with the rise of the heat source parameter.
- Magnifying viscous dissipation producing the additional energy, which encourages the temperature.
- The temperature profile is reducing with an increase of radiation parameter, coupling parameter, magnetic field.
- The heat transfer rate of nanofluid against frequency parameter is increasing with an improvement of the Eckert number.
- The heat transfer is decreasing with an increase of Rd, ϕ, K, and M.

References

1. S.M. Abo-Dahab, M.A. Abdelhafez, F. Mebarek-Oudina, S.M. Bilal, MHD Casson nanofluid flow over nonlinearly heated porous medium in presence of extending surface effect with suction/injection, *Indian J. Phys.*, **95**:2703–2717, 2021, `https://doi.org/10.1007/s12648-020-01923-z`.

2. A.R. Bestman, Pulsatile flow in a heated porous channel, *Int. J. Heat Mass Transfer*, **25**(5):675–682, 1982, `https://doi.org/10.1016/0017-9310(82)90172-7`.

3. A. Bhattacharyya, G.S. Seth, R. Kumar, A.J. Chamkha, Simulation of Cattaneo–Christov heat flux on the flow of single and multi-walled carbon nanotubes between two stretchable coaxial rotating disks, *J. Therm. Anal. Calorim.*, **139**(3):1655–1670, 2020, `https://doi.org/10.1007/s10973-019-08644-4`.

4. P. Bitla, T.K.V. Iyengar, Pulsating flow of an incompressible micropolar fluid between permeable beds, *Nonlinear Anal. Model. Control*, **18**:399–411, 2013, `https://doi.org/10.15388/NA.18.4.13969`.

5. P. Bitla, T.K.V. Iyengar, Pulsating flow of an incompressible micropolar fluid between permeable beds with an inclined uniform magnetic field, *Eur. J. Mech. B. Fluids*, **48**:174–182, 2014, `https://doi.org/10.1016/j.euromechflu.2014.06.002`.

6. A.J. Chamkha, Flow of two-immiscible fluids in porous and nonporous channels, *J. Fluids Eng.*, **122**(1):117–124, 2000, `https://doi.org/10.1115/1.483233`.

7. A.J. Chamkha, T. Grosan, I. Pop, Fully developed free convection of a micropolar fluid in a vertical channel, *Int. Commun. Heat Mass Transfer*, **29**(8):1119–1127, 2002, `https://doi.org/10.1016/S0735-1933(02)00440-2`.

8. S.U.S. Choi, Nanofluid technology: Current status and future research, in *Korea–U.S. Technical Conference on Strategic Technologies, October 22–24, 1998, Vienna, VA*, Argonne National Lab., Argonne, IL, 1998, pp. 1–23, `https://www.osti.gov/servlets/purl/11048`.

9. S.U.S. Choi, J.A. Eastman, Enhancing thermal conductivity of fluids with nanoparticles, in *ASME International Mechanical Engineering Congress and Exposition, November 12–17, 1995, San Francisco, CA*, ASME, New York, 1995, pp. 99–105, `https://www.osti.gov/servlets/purl/196525`.

10. S. EL-Kabeir, A.M. Rashad, W. Khan, Z.M. Abdelrahman, Micropolar ferrofluid flow via natural convective about a radiative isoflux sphere, *Adv. Mech. Eng.*, **13**(2):1–10, 2021, `https://doi.org/10.1177/1687814021994392`.

11. N.S. Elgazery, Flow of non-Newtonian magneto-fluid with gold and alumina nanoparticles through a non-Darcian porous medium, *J. Egypt. Math. Soc.*, **27**(1):1–25, 2019, `https://doi.org/10.1186/s42787-019-0017-x`.

12. A. Eringen, Theory of micropolar fluids, *Indiana Univ. Math. J.*, **16**(1):1–18, 1966, `https://doi.org/10.1512/iumj.1967.16.16001`.

13. A.C. Eringen, Theory of thermo-microstretch fluids and bubbly liquids, *Int. J. Eng. Sci.*, **28**(2):133–143, 1990, `https://doi.org/10.1016/0020-7225(90)90063-O`.

14. M.M. Hashmi, T. Hayat, A. Alsaedi, On the analytic solutions for squeezing flow of nanofluid between parallel disks, *Nonlinear Anal. Model. Control*, **17**(4):418–430, 2012, `https://doi.org/10.15388/na.17.4.14048`.

15. M. Hatami, J. Hatami, D.D. Ganji, Computer simulation of MHD blood conveying gold nanoparticles as a third grade non-Newtonian nanofluid in a hollow porous vessel, *Comput. Methods Programs Biomed.*, **113**(2):632–641, 2014, `https://doi.org/10.1016/j.cmpb.2013.11.001`.

16. C.K. Kumar, S. Srinivas, A. Subramanyam Reddy, MHD pulsating flow of Casson nanofluid in a vertical porous space with thermal radiation and Joule heating, *J. Mech.*, **36**(4):535–549, 2020, `https://doi.org/10.1017/jmech.2020.5`.

17. A. Mahdy, E.R. El-Zahar, A.M. Rashad, W. Saad, H.S. Al-Juaydi, The magneto-natural convection flow of a micropolar hybrid nanofluid over a vertical plate saturated in a porous medium, *Fluids*, **6**(6), 2021, `https://doi.org/10.3390/FLUIDS6060202`.

18. F. Mebarek-Oudina, Convective heat transfer of titania nanofluids of different base fluids in cylindrical annulus with discrete heat source, *Heat Transfer Asian Res.*, **48**(1):135–147, 2019, `https://doi.org/10.1002/htj.21375`.

19. F. Mebarek-Oudina, R. Bessaih, B. Mahanthesh, A.J. Chamkha, J. Raza, Magneto-thermal-convection stability in an inclined cylindrical annulus filled with a molten metal, *Int. J. Numer. Methods Heat Fluid Flow*, **31**(4):1172–1189, 2021, `https://doi.org/10.1108/HFF-05-2020-0321`.

20. A.J. Chamkha M.V. Krishna, Hall and ion slip effects on MHD rotating flow of elastico-viscous fluid through porous medium, *Fluids*, **113**:104494, 2020, `https://doi.org/10.1016/j.icheatmasstransfer.2020.104494`.

21. G. Radhakrishnamacharya, M.K. Maiti, Heat transfer to pulsatile flow in a porous channel, *Int. J. Heat Mass Transfer*, **20**(2):171–173, 1977.

22. C. Rajashekhar, F. Mebarek-Oudina, H. Vaidya, K. V. Prasad, G. Manjunatha, H. Balachandra, Mass and heat transport impact on the peristaltic flow of a Ree–Eyring liquid through variable properties for hemodynamic flow, *Heat Transfer*, **50**(5):5106–5122, 2021, `https://doi. org/10.1002/htj.22117`.

23. A.M. Rashad, S. Abbasbandy, A.J. Chamkha, Mixed convection flow of a micropolar fluid over a continuously moving vertical surface immersed in a thermally and solutally stratified medium with chemical reaction, *J. Taiwan Inst. Chem. Eng.*, **45**(5):2163–2169, 2014, `https: //doi.org/10.1016/j.jtice.2014.07.002`.

24. A.M. Rashad, W.A. Khan, S.M.M. EL-Kabeir, A.M.A.EL-Hakiem, Mixed convective flow of micropolar nanofluid across a horizontal cylinder in saturated porous medium, *Appl. Sci.*, **9**(23), 2019, `https://doi.org/10.3390/app9235241`.

25. A.M. Rashad, W.A. Khan, I. Tlili, A.M.A. EL-Hakiem, Unsteady slip flow of a micropolar nanofluid over an impulsively stretched vertical surface, *Indian J. Pure Appl. Phys.*, **57**(10):773–782, 2019.

26. F. Selimefendigil, H.F. Oztop, A.J. Chamkha, Role of magnetic field on forced convection of nanofluid in a branching channel, *Int. J. Numer. Methods Heat Fluid Flow*, **30**(4):1755–1772, 2020, `https://doi.org/10.1108/HFF-10-2018-0568`.

27. M. Sheikholeslami, M. Hatami, D.D. Ganji, Micropolar fluid flow and heat transfer in a permeable channel using analytical method, *J. Mol. Liq*, **194**:30–36, 2014, `https: //doi.org/10.1016/j.molliq.2014.01.005`.

28. S. Srinivas, C.K. Kumar, A.S. Reddy, Pulsating flow of casson fluid in a porous channel with thermal radiation, chemical reaction and applied magnetic field, *Nonlinear Anal. Model. Control*, **23**(2):213–233, 2018, `https://doi.org/10.15388/NA.2018.2.5`.

29. A. Subramanyam Reddy, S. Srinivas, K. Jagadeshkumar, Blood-gold/coppernanofluid flow between expanding or contracting permeable walls with slip effects, *Mater. Today Proc.*, **9**:351– 360, 2019, `https://doi.org/10.1016/j.matpr.2019.02.164`.

30. T. Tayebi, A.J. Chamkha, Magnetohydrodynamic natural convection heat transfer of hybrid nanofluid in a square enclosure in the presence of a wavy circular conductive cylinder, *J. Therm. Sci. Eng. Appl.*, **12**(3):031009, 2020, `https://doi.org/10.1115/1.4044857`.

31. G. Venkatesan, A.S. Reddy, Insight into the dynamics of blood conveying alumina nanoparticles subject to Lorentz force, viscous dissipation, thermal radiation, Joule heating, and heat source, *Eur. Phys. J. Spec. Top.*, **230**:1475–1485, 2021, `https://doi.org/10. 1140/epjs/s11734-021-00052-w`.

32. A. Vijayalakshmi, S. Srinivas, B. Satyanarayana, A. Subramanyam Reddy, Hydromagnetic pulsating flow of nanofluid between two parallel walls with porous medium, *Mater. Today Proc.*, **9**:306–319, 2019, `https://doi.org/10.1016/j.matpr.2019.02.161`.

33. C.Y. Wang, Pulsatile flow in a porous channel, *J. Appl. Mech.*, **38**(2):553–555, 2017, `https: //doi.org/10.1115/1.3408822`.